BCSIR

Available online at www.banglajol.info

Bangladesh J. Sci. Ind. Res. **54(4)**, 289-296, 2019

BANGLADESH JOURNAL OF SCIENTIFIC AND INDUSTRIAL RESEARCH

E-mail: bjsir07@gmail.com

Influence of NaCl on the formation of stoichiometric polycrystalline $La_{0.85}Na_{0.15}MnO_3$

R. Majumder[1], M. M. Hossain[2], M. E. Hossain[1] and M. A. R. Sarker[3]*

[1]*Physics Discipline, Khulna University, Khulna 9208, Bangladesh*

[2]*Industrial Physics Division, Bangladesh Council of Scientific and Industrial Research (BCSIR), Dhaka 1205, Bangladesh*

[3]*Department of Physics, University of Rajshahi, Rajshahi 6205, Bangladesh*

Abstract

Origination of defects and loss of Na during the sintering process are the major problems for the conventional solid-state synthesis technique to form sodium (Na) doped lanthanum manganite. To minimize defect and Na loss during the sintering process, the sodium (Na) doped lanthanum manganite with 15% substitution of La by Na ($La_{0.85}Na_{0.15}MnO_3$) was synthesized using the NaCl flux material incorporated with the conventional solid-state reaction technique (flux method). The amount of micro strain, lattice strain and dislocation density for the flux method to grow polycrystalline $La_{0.85}Na_{0.15}MnO_3$were detected successfully. The structural study using X-ray diffraction (XRD), Fourier transform infrared spectroscopy (FTIR), Scanning Electron Microscopy (SEM) and Energy Dispersive Analysis X-Ray (EDAX) showed that the use of flux synthesis technique instead of conventional solid-state reaction technique was satisfactory to obtain stoichiometric $La_{0.85}Na_{0.15}MnO_3$ polycrystalline structure with a smaller defect. From the closer inspection of the XRD spectrum for $La_{0.85}Na_{0.15}MnO_3$ significantly showed a higher order layered structure for the cathode material for using this flux technique, which is a very important feature to increase the efficiency of the cathode material.

Received: 06 October 2018

Revised: 16 January 2019

Accepted: 06 May 2019

DOI: https://doi.org/10.3329/bjsir.v54i4.44563

Keywords: $La_{0.85}Na_{0.15}MnO_3$; Flux method; Structural properties

Introduction

Over the few decades the investigation of monovalent Na doping on lanthanum manganite system has become very popular for its numerous application and research for device fabrication (Roy *et al*., 2001; Rao *et al.,* 1999; Ehi-Eromosele *et al*., 2015; Lakshmi *et al.,* 2009; Malavasi *et al*., 2003; Kansara *et al*., 2015; Malavasi *et al*., 2003). Na-doped lanthanum manganites have large Tc as well as large magnetoresistance values near room temperature which nominates this compound as encouraging materials for information technologies, medicine and low-temperature thermal engineering (Ehi-Eromosele *et al*., 2015). Hence, it is desirable to study this promising compound at different point of views. The dependence of the physical and chemical properties like the order of crystallinity, band gap, optical absorption, electrochemical performance of cathode materials directly related to the perfection of crystalline structure. To obtain the better crystalline structure with minimum defects, we are always motivated to the study of new synthesis routes to produce our desired materials. There are several widely used methods to form a material with crystalline or polycrystalline structure. Among all, the most common and easier technique is the solid-state reaction technique. But the major problem for the conventional solid-state reaction technique to grow Na doped lanthanum manganite is the loss of Na, during sintering process (Rao *et al*., 1999; Ehi-Eromosele *et al*., 2015). Moreover, in solid-state reaction technique, the addition of impurity and dirt can be originated during long sintering process thus larger defect and thermal strain in the crystal structure can be occurred. To provide a clean environment for the crystal growth with fewer defects and less thermal strain, salt flux materials

*Corresponding author e-mail: razzaqueru2000@gmail.com

(NaCl/KCl) are used widely all over the world (Ozawa and Kauzlarich, 2003; Brylak *et al*., 1995; Nientiedt *et al*., 1997; Nientiedt and Jeitschko, 1998). Using flux material together with target compound can protect dirt, impurities, and oxides away from the surface of the molten composite material. It acts as if there were a vacuum container surrounding the molten material. Thus protects the molten material from further contamination of crucible or other impurities originate during long sintering process and minimize the loss of Na due to oxidation. Hence introducing flux material in conventional solid-state reaction technique pure crystalline phase with proper doping content can be achieved. In this study, we have used flux method taking NaCl salt as flux material incorporated with conventional solid-state reaction. C. O. Ehi-Eromosele *et al*. got the highest crystallinity for the doping amount of x= 0.15 in their observation (Ehi-Eromosele *et al*., 2015). So in our present work, the value of Na doping content x= 0.15 has been chosen to ensure the high crystallinity of the sample.

Materials and methods

Sample preparation

For the preparation of $La_{0.85}Na_{0.15}MnO_3$ sample using flux method, high-purity (>99.9%) powders of La_2O_3, NaCl and MnO_2 were used as the starting material. Initially, we studied the phase formation with the help of thermal gravimetric analysis (TG/DTA) in order to get precious guideline for the synthesizing of $La_{0.85}Na_{0.15}MnO_3$. At the first step of the synthesis, a stoichiometric powder mixture of La_2O_3, NaCl, and MnO_2 was assorted competently using ethanol in an agate mortar and then the reactants were dried in an oven in an air atmosphere at 200°C for 12h.Then excess NaCl was added as a flux material in 10 times of precursor. Thus the obtained powder calcined at 900°C for 24h in an air atmosphere for flux growth. The polycrystalline $La_{0.85}Na_{0.15}MnO_3$ sample was obtained in the solid form surrounded by flux material. The flux material was washed by hot water for several times and $La_{0.85}Na_{0.15}MnO_3$ powder was obtained by filtration. The powder sample was pelletized in 8 mm diameter under a pressure of 60KN using pressure gauge. The temperature rising and cooling rates were 2°C per minute in all the heat treatments procedure.

Characterization methods

The powder sample was analyzed in the range of diffraction angle (2θ) between 20° and 80° by X-ray diffraction (BRUKER D8 advance, Germany) using a CuKα (λ= 0.154 nm) radiation source at room temperature. Fourier Transform Infrared Spectroscopy (FTIR) measurement of the sample was performed in the wave number range 400-4000 cm^{-1} using the model Nicolet-6700. A Scanning Electron Microscope (SEM: 6490 JEOL JSM) was used to analyze the surface morphology of the synthesized sample. The Energy Dispersive Analysis X-Ray (EDAX) attached with 6490 JEOL JSM model scanning electron microscope was performed to confirm stoichiometric composition.

Results and discussion

Thermal analysis

TG/DTA profile of the thermal decomposition of $La_{0.85}Na_{0.15}MnO_3$ sample is shown in Fig. 1. The weight loss of the sample has been accomplished stepwise in the temperature range 30-964°C. Above 964°C, there was no weight change and the phase formation was complete. This initially provided precious guidance for choosing proper sintering temperature of this composite system. The initial weight loss takes place between 30°C and 70°C due to evaporation of ethanol and moisture and the observed weight loss was about 5%. The observed bands in the FTIR spectrum in the range 3300-3800 cm^{-1} confirms the presence of moisture and ethanol in the sample can be diminished with the sintering [figure 3]. The weight loss in 354-577 °C is about 5.67% and then there is roughly a sudden change in weight is observed between 577-964 °C with a weight loss of about 10.82%. The weight losses in this prominent region are the consequence of the reduction of oxygen, the liberation of Cl_2 and decomposition of raw materials respectively. On the differential thermal analysis (DTA) profile of this sample indicates one strong endothermic effect in the range 30-70°C (minimum at ~ 59°C), two strong endothermic effects in the range 354-460°C (minimum at ~ 384 and 424°C) and three minor endothermic effects in the range 460-964°C (minimum at ~ 636, 769 and 899.8°C). This reveals a strong confirmation of the TG curve with an indication that our sample is thermally stable above 964°C and hence a good candidate for high-temperature applications. For the energy storage and conversion devices where inserted cathode needs to be stable above a certain temperature (1000°C), $La_{0.85}Na_{0.15}MnO_3$ can be used effectively.

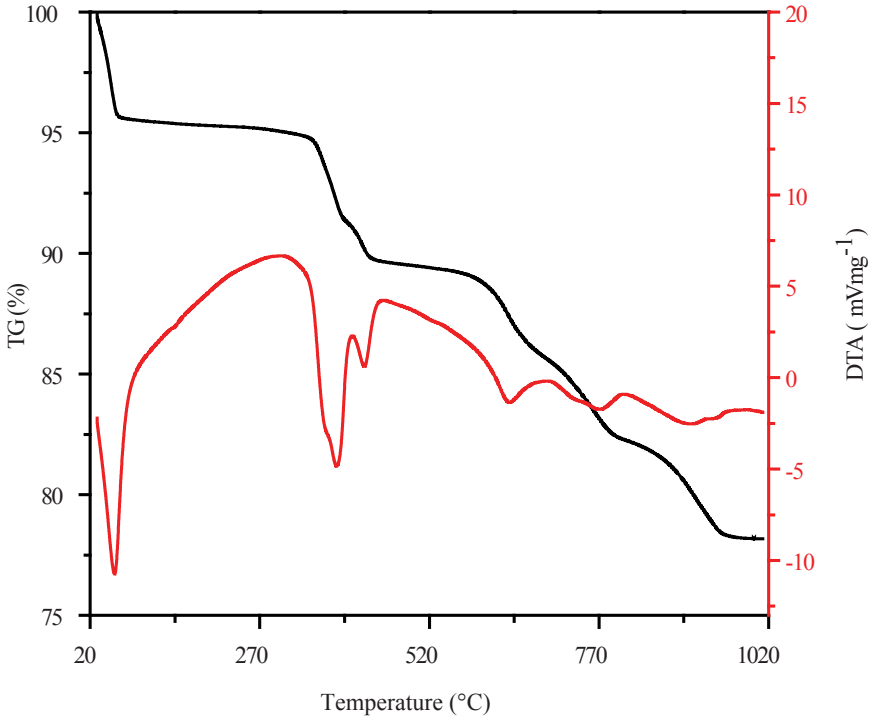

Fig. 1. The TG/DTA curves for the phase formation and thermal decomposition of $La_{0.85}Na_{0.15}MnO_3$ sample

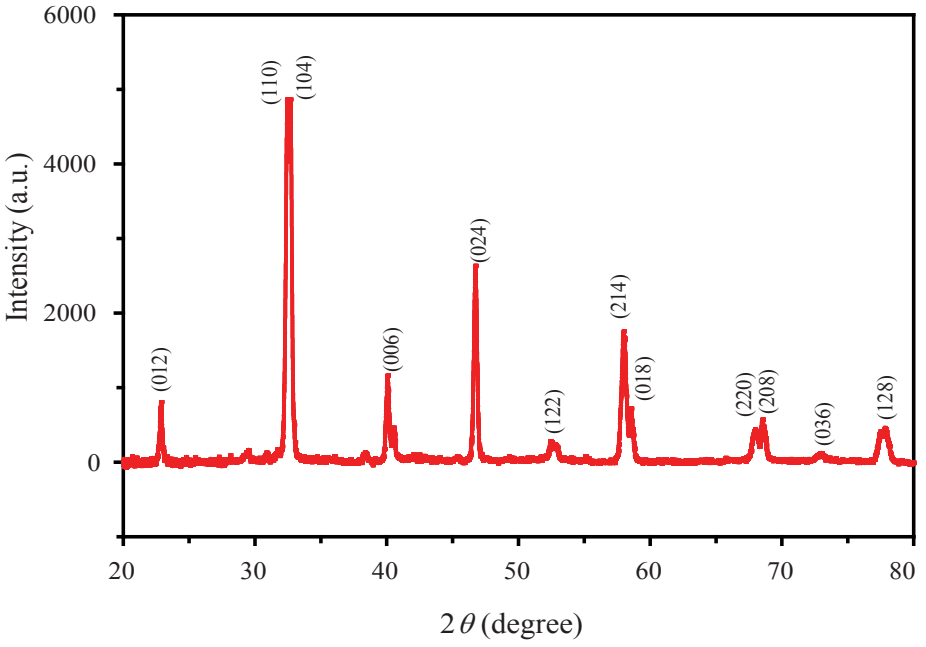

Fig. 2. The X-ray diffraction pattern for the $La_{0.85}Na_{0.15}MnO_3$ sample

Structural analysis

X-ray diffraction (XRD)

Typical XRD pattern for $La_{0.85}Na_{0.15}MnO_3$ powder indexing with JCPDS data No. 50-0298 is shown in Fig. 2, which reveals that the prepared sample belongs to the homogeneous single phase rhombohedral perovskites crystal structure with the space group of R-3c.

The powder sample was characterized at room temperature by an X-ray diffractometer in the range from 2θ= 20° to 80° with CuK_α radiation (λ= 1.5418Å), at 40KV and 30mA. XRD data incorporated with cell cal software provides structural parameters from the refinement of the hexagonal unit cell for the $La_{0.85}Na_{0.15}MnO_3$ sample. Observed sharp peaks in the XRD pattern indicate the good crystallinity of the sample with no impurity phase peaks of La_2O_3, NaCl, and MnO_2 confirms the single phase powder was obtained. In this work, the rhombohedral perovskites structure of $La_{0.85}Na_{0.15}MnO_3$ having lattice parameters $a=b$= 5.504 Å, c=13.37 Å, and unit cell volume 350.89 Å^3 are consistent with reported values for doping amount x= 0.15 (Lakshmi *et al.,* 2009; Malavasi *et al.*, 2003; Kansara *et al.,* 2015). From the closer inspection of the XRD spectrum shows doublet peaks in the pattern for doping amount of x= 0.15. Splitting of the (110)/(104), (214)/(108) and (220)/(208) doublets near 32.5, 58 and 68° indicated a highly ordered layered structure for the cathode materials (Xiao *et al.,* 2017). The salient properties of a crystalline material like electrochemical performance, the performance of SOFCs and cation ordering in the cathode material extensively depend on the perfection of crystallinity. The perfection of crystallinity can be measured by the intensity ratio, grain size (D), microstrain ($\mathcal{E}$), lattice strain and dislocation density (δ) (Yilmaz *et al.,* 2012; Rajasekar *et al.*, 2008). Here the dislocation density (δ) is the length of dislocation lines per unit volume and is the measure of the amount of the defects in a crystal. The average grain size (D), microstrain ($\mathcal{E}$) and dislocation density (δ) of the $La_{0.85}Na_{0.15}MnO_3$ crystalline powder were calculated using

$$D = \frac{0.9\lambda}{\beta \cos\theta} \qquad (1)$$

$$\varepsilon = \frac{\beta \cos\theta}{4} \qquad (2)$$

$$\delta = \frac{1}{D^2} \qquad (3)$$

equation (1), (2) and (3) respectively, where 0.9, λ, β and θ are indicating the crystal shape constant, X-ray wavelength (1.54Å), full width at half maximum (FWHM) of the highest peak in radians and reflection angle of the highest peak respectively (Yilmaz *et al.,* 2012; Rajasekar *et al.,* 2008).

Table I. Intensity ratio of the largest two peaks, grain size, dislocation density, microstrain and lattice strain derived from x-ray diffraction data

Parameters	Values
Intensity ratio, I_{104}/I_{024}	1.877
Grain Size, D(nm)	21.29
Dislocation density, δ x 10^{14} (lines.m^{-2})	22.06
Microstrain, $\mathcal{E}$	0.162
Lattice Strain	0.006

The calculated values of I_{110}/I_{024}, D, δ, $\mathcal{E}$ and lattice strain for the flux synthesis technique are listed in Table I. The values of intensity ratio, grain size, dislocation density, microstrain and lattice strain in the present study are in good agreement with the available experimental data and ensure the better ability of flux method to form higher order crystalline structure for the $La_{0.85}Na_{0.15}MnO_3$ system with smaller defect. Moreover highly ordered layered structure and higher order crystallinity for the cathode materials ensures the better electrochemical performance of $La_{0.85}Na_{0.15}MnO_3$ sample and can be used as novel electrode materials for advanced energy conversion and storage battery devices prolonging the cycle life of rechargeable batteries.

Fourier transforms infrared spectroscopy (FTIR) analysis

The FTIR spectrum of $La_{0.85}Na_{0.15}MnO_3$ is shown in Fig. 3. As seen from the figure, the most significant absorption bands are located around 478, 605, 651, 954, 1097, 1477, 1624, 2862, 2927, 3452 and 3693 cm^{-1}. The three characteristics absorption bands of the FTIR spectrum of $La_{0.85}Na_{0.15}MnO_3$ are located at 478, 605 and 651 cm^{-1}.The absorption peaks at 478 cm^{-1} correspond to the vibration for La-O bond (Berger *et al.,* 2013). The absorption band around 605 and 651 cm^{-1} representing a significant stretching mode of vibration of the Mn-O bond, due to an internal motion of the Mn-ion against the oxygen octahedron and deformation of bound O-Mn-O bond length respectively (Kim *et al*., 1996). This confirms the XRD data showing that the vibration bands for precursors vanished and the vibration bands for oxide network developed within the expected perovskites structure. The bands around 1097 and 954 cm^{-1} are the consequence of C-O vibration bond estimated due to the use of ethanol in the mixing process of raw materials and

calcinations of the sample in the air atmosphere for a high range of temperature. A broad absorption band around 3452 cm^{-1} corresponds to the vibration of O-H and La-OH bonds originated from the similar fact of the previous discussion (Hernándeza *et al*., 2015). The absorption band around 1477 cm^{-1} due to the $LaCO_3$ can be decreased with sintering (Gupta

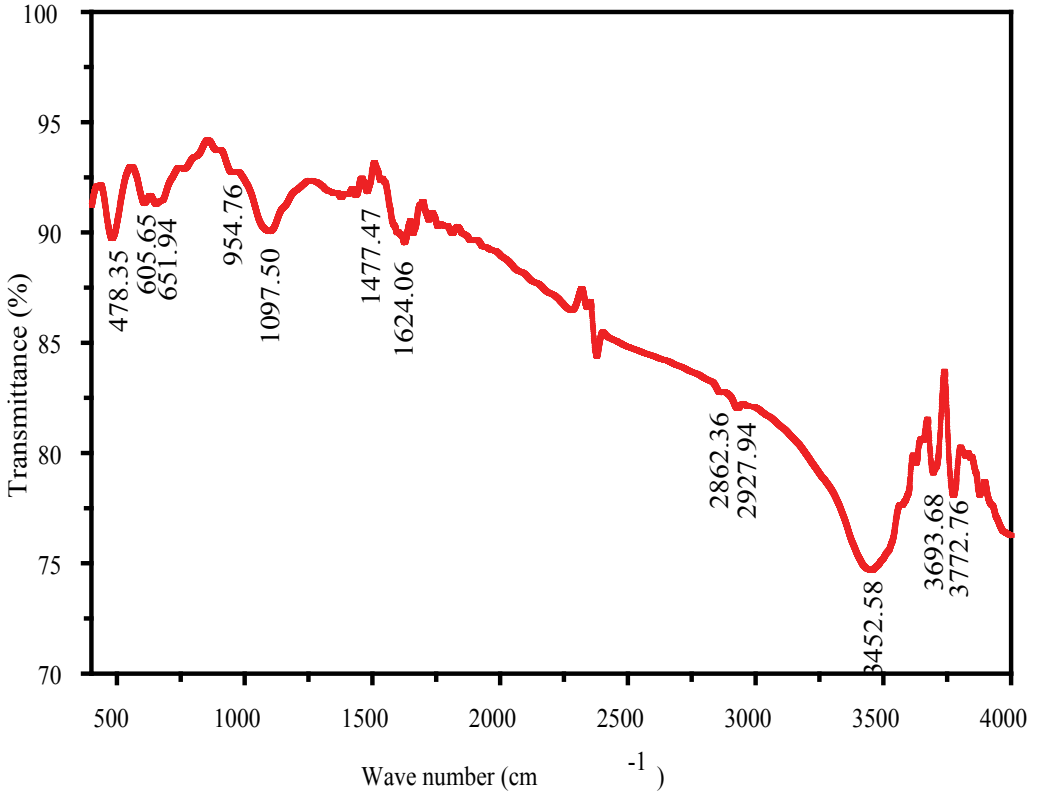

Fig. 3. FTIR spectrum for $La_{0.85}Na_{0.15}MnO_3$ sample

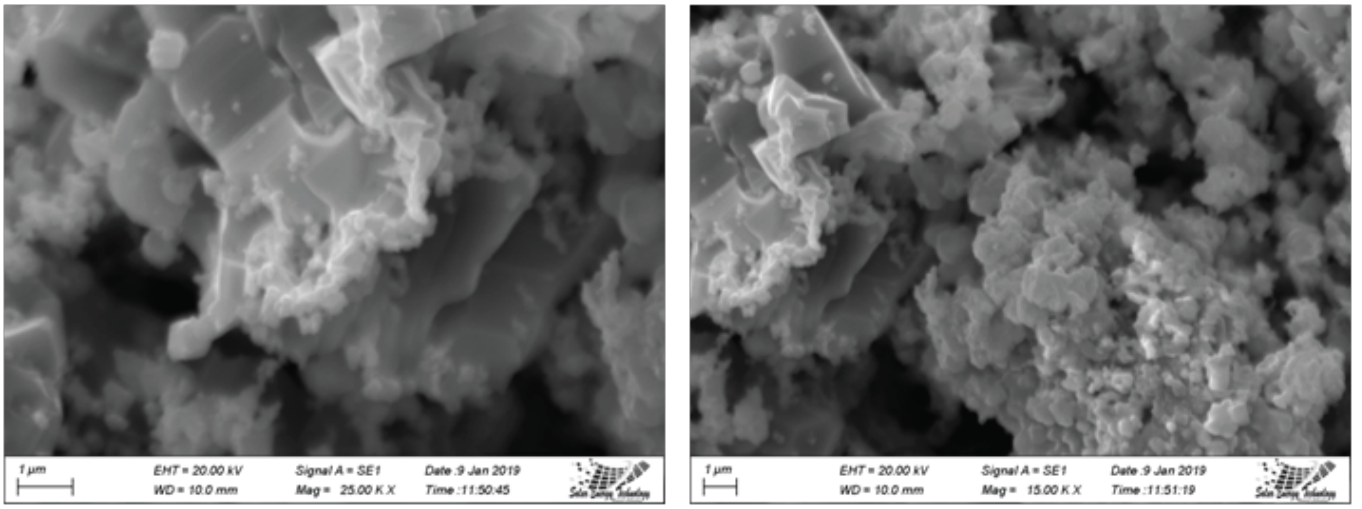

Fig. 4. Scanning electron microscopy for $La_{0.85}Na_{0.15}MnO_3$

et al., 2012). Finally, the absorption peaks near 2862 and 2927 cm^{-1} are the signatures of vibration of C-H bond and the range 3600–3700 cm^{-1} corresponds to the vibration of O–H bond due to moisture and ethanol. The FTIR spectrum clearly identifies the functional groups of active compound, their corresponding bands and oxide network formation in the synthesized $La_{0.85}Na_{0.15}MnO_3$ sample.

Scanning electron microscopy (SEM)

To investigate the surface morphology scanning electron microscopy (SEM) was performed. Figure 4 indicates the surface morphology and particle distribution of $La_{0.85}Na_{0.15}MnO_3$. From the entire figure, it is observed that particles of this sample have high distribution and heterogeneous shape.

Energy dispersive analysis X-ray (EDAX)

Energy dispersive analysis X-ray (EDAX) or some time refers to EDS/EDX is an X-ray spectroscopic method for the determination of elemental composition of a material.

To confirm the chemicaland stoichiometric composition for $La_{0.85}Na_{0.15}MnO_3$, EDAX was performed and represented in Fig. 5.

This EDAX spectrum reveals that all the constituent elements of $La_{0.85}Na_{0.15}MnO_3$ (La, Na, Mn, and O) are present in our prepared sample. From EDAX spectrum it can be also noticed that no impurity element signals are present throughout the whole spectrum. This is indicative to the less origination of impurity for the flux synthesis

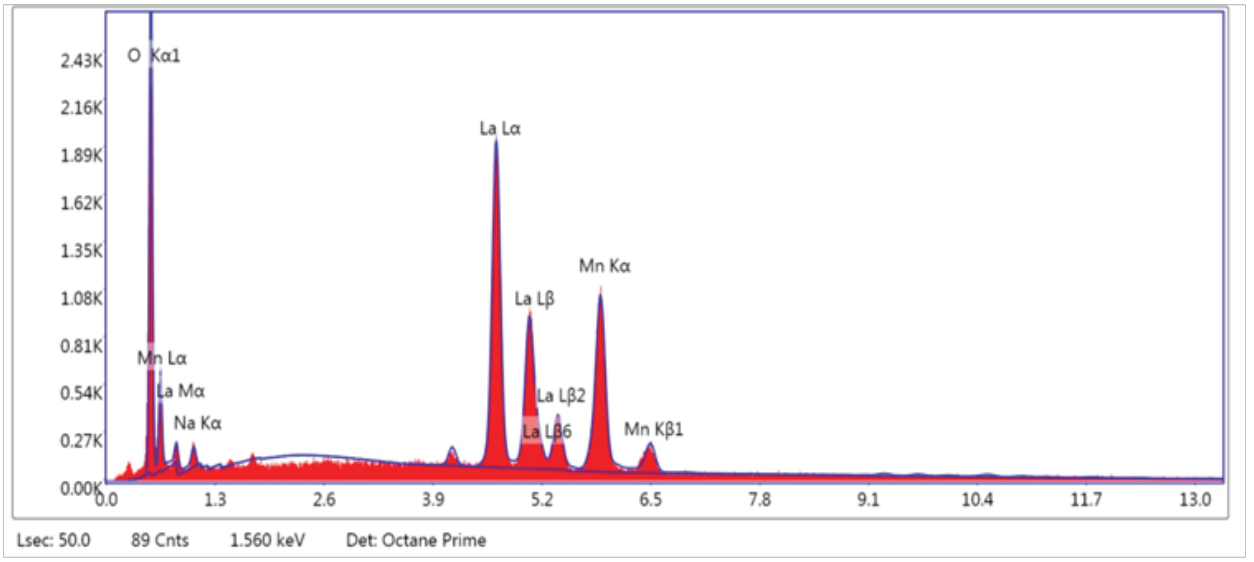

Fig. 5. EDAX spectrum of $La_{0.85}Na_{0.15}MnO_3$

Table II. Composition of $La_{0.85}Na_{0.15}MnO_3$ with elemental percentage stoichiometry

Element	Weight percentage	Atomic Percentage
Oxygen, O	16.95	54.37
Sodium, Na	1.35	3.01
Lanthanum, La	59.66	22.04
Manganese, Mn	22.04	20.58

technique. The elemental composition and constituent percentages in $La_{0.85}Na_{0.15}MnO_3$ are listed in Table II, which is consistent with the EDAX spectrum and represents the compatible stoichiometry for 15% Na substituted lanthanum manganite.

Conclusion

The homogeneous stoichiometric polycrystalline powder of $La_{0.85}Na_{0.15}MnO_3$ was successfully synthesized by flux method. The phase formation condition in synthesized profile was demonstrated by thermal analysis and crystalline phase was confirmed by X-ray diffraction study. The stoichiometric composition for $La_{0.85}Na_{0.15}MnO_3$ sample was confirmed using EDAX, which also revealed the better ability of the flux method to grow polycrystalline $La_{0.85}Na_{0.15}MnO_3$without any noticeable impurity elements. The higher value of intensity ratio, a smaller value of dislocation density and microstrain were in good agreement with the result of EDAX spectrum and alternatively substantiated efficiency of flux method.

Acknowledgement

This work was partially supported by the Khulna University Research Cell (Khubi/Gacell-04/2000-13). Authors would like to thank Khulna University authority for providing funds under the university research project to carry out this work. The authors like to thank Mr. Karimul Hoque, Assistant Professor, Physics Discipline, Khulna University and Mr. Md. Khairul Amin, Assistant Professor, Chemistry Discipline, Khulna University for their cooperation and suggestion during this research work.

References

Berger D, Van Landschot N, Ionica C, Papa F and Fruth V (2013), Synthesis of pure and doped lanthanum cobaltite by the combustion method, *J OptoelectronAdv Matter* **5:**719.

Brylak M, Möller MH and Jeitschko WJ (1995), Ternary ArsenidesACuAs$_2$ and Ternary AntimonidesAAgSb$_2$ (A = Rare-Earth Elements and Uranium) with HfCuSi$_2$-Type structure, *Solid State Chem*. **115:** 305.

Ehi-Eromosele CO, Ita BI, Ajanaku KO, Edobor-Osoh A, Aladesuyi O, Adalikwu SA and Ehi-Eromosele FE (2015), Structural, morphological and magneticproperties of $La_{1-x}NayMnO_3$ ($y \leq x$) nanoparticles produced by the solutioncombustion method, *Bull Mater Sci*. **38 (7):** 1749–1755.

Gupta M, Khan W, Yadav P, Kotnala RK, Azam A and Naqvi AH (2012), Synthesis and evolution of magnetic properties of Ni doped $La_{2/3}Sr_{1/3}Mn_{1-x}Ni_xO_3$ nanoparticles, *J Appl Phys*. **111:** 093-706.

Hernándeza E, Sagredoa V and Delgado GE (2015), Synthesis and magnetic characterization of $LaMnO_3$ nanoparticles, *Rev Mex Fis*. **61:** 166–169.

Kansara SB, Dhruva D, Kataria B, Thaker CM, Rayaprol S, Prajapat CL, Singhc MR, Solanki PS, Kuberkar DG and Shaha NA (2015), Structural, transport and magnetic properties of monovalent Doped $La_{1-x}Na_xMnO_3$ manganites, *Ceram Int*. **41:** 7162-7173. DOI: org/10.1016/j.ceramint.2015.02.037

Kim KH, Gu JY, Choi HS, Park GW and Noh TW (1996), Frequency shifts of the internal phonon modes in $La_{0.7}Ca_{0.3}MnO_3$, *Phys Rev Lett*. **77:**9. DOI:https://doi.org/10.1103/PhysRevLett.77.1877

Lakshmi YK, Venkataiah G and Venugopal Reddy P (2009), Magnetoelectric behavior of sodium doped lanthanum manganites, *J Appl. Phys*. **106:** 023-707. DOI: org/10.1063/1.3173285

Malavasi L, Mozzati MC, Polizzi S, Azzoni CB, and Flor G (2003), Nanosized sodium-doped lanthanum manganites: Role of the synthetic route on their physical properties, *Chem Mater*. **15:** 5036- 5043. DOI: org/10.1021/cm0311271

Malavasi L, Mozzati MC, Ghigna P, Azzoni CB and Flor (2003), Lattice disorder, electric properties and magnetic behavior of $La_{1-x}Na_xMnO_{3+\delta}$ manganites, *J Phys Chem B*. **107:** 2500. DOI: org/10.1021/jp027015z

Nientiedt AT, Jeitschko W, Pollmeier PG and Brylak, MZ (1997), Quaternary equiatomic manganese pnictide oxides AMnPO (A = La-Nd, Sm, Gd-Dy), AMnAsO (A = Y, La-Nd, Sm, Gd-Dy, U) and AMnSbO (A = La-Nd, Sm, Gd) with ZrCuSiAs type structure, *Naturforsch* **52b:** 560.

Nientiedt AT and Jeitschko W (1998), Equiatomic quaternary Rare Earth Element Zinc pnictide Oxides RZnPO and

RZnAsO, *Inorg Chem*. **37:** 386. DOI: org/10.1021/ic971058q

Ozawa TC and Kauzlarich SM (2003), Flux single crystal growth and crystal structure of the new quaternary mixed-metal pnictide: $BaCuZn_3As_3$, *Inorganic Chemistry* **42(10):** 3183-3186. DOI: org/10.1021/ic034061k

Rajasekar K, Kungumadevi L, Subbarayan L, Sathyamoorthy R (2008), Thermal sensors based on Sb_2Te_3 and $(Sb_2Te_3)_{70}(Bi_2Te_3)_{30}$ thin films, *Ionics* **14:** 69.

Rao G H, Sun J R, Barner K and Hamad N (1999), Crystal structure and magnetoresistance of Na-doped $LaMnO_3$, *J Phys: Condens Matter*. **11:** 1523–1528.

Roy S, Guo YQ, Venkatesh S and Ali N (2001), Interplay of structure and transport properties of sodium-doped lanthanum manganite, *J Phys: Condens Matter*. **13:** 9547–9559.

Xiao P, Lv T J, Chen X and Chang C (2017), $LiNi_{0.8}Co_{0.15}Al_{0.05}O_2$: Enhanced electrochemical performance from reduced cationic disordering in Li slab, *Sci Rep*,**7:** 1408.

Yilmaz M, Turgut G and Aydin S (2012), Structures by spray pyrolysis technique for rechargeable Li-ion battery, *J ChemSoc Pak*. **34:** 283.